Methods to Optimize Plasmonic Structure Integrated Single-Photon Detector Designs

Mária Csete[*1], Gábor Szekeres[1], Balázs Bánhelyi[2], András Szenes[1], Tibor Csendes[2] and Gábor Szabó[1]
[1]Department of Optics and Quantum Electronics, University of Szeged, H-6720 Szeged, Dóm tér 9,
[2]Department of Computational Optimization, University of Szeged, H-6720 Szeged, Árpád tér 2, Hungary
*Corresponding author: mcsete@physx.u-szeged.hu

Abstract: Novel methodology was implemented using LiveLink for MATLAB to maximize the absorptance of superconducting nanowire single photon detectors in conical mounting by optimizing device configurations in COMSOL RF module. In this paper reference devices are compared to devices determined by Monte-Carlo and Nelder-Mead optimizing algorithms built in COMSOL and to devices determined by GLOBAL optimization method. Optimization was realized on three detector designs in two steps, when the geometry was partially-, and completely varied. In every case the polar angle dependent absorptance and the spectral sensitivity was also inspected. These results show that the highest absorptances can be reached via complete optimization performed via GLOBAL. Namely, ~1.3% (74.96 from 73.66%) absorption improvement is achieved in NCAI-SNSPD, and in NCDAI-SNSPD and NCDDAI-SNSPD ~15.12% (93.34 from 78.22%) and ~7.5% (94,34 from 86.84%) absorptance increase is attainable with respect to the reference devices.

Keywords: Single-photon detectors, Surface plasmon polaritons, Plasmonics, Optimization.

1. Introduction

Predesigned plasmonic structures are capable of enhancing various optical phenomena, the key concept is to engineer the spectral response and the accompanying near-field distribution by tailoring the integrated devices' composition [1]. A growing application area is improvement of superconducting nanowire single-photon detector's (SNSPDs) detection efficiency, which is important in quantum information processing [2-14]. The low absorptance of simple devices based on bare patterns of superconducting nanowires [2] was improved by optical cavities [3-5], novel superconducting materials [6, 7] and via waveguide coupling [8]. Competitive absorptance enhancement was achieved via integrated plasmonic structures [9-12]. Our previous studies have shown that three-quarter-wavelength periodic plasmonic structures are capable of significantly improving detection efficiency [11, 12]. The advantage of these devices is that high absorptance can be achieved, while short reset time is ensured via reduced wire lengths. In our previous studies parametric sweep method in RF module of COMSOL was used to determine the optimal orientations of different plasmonic structure integrated detectors, where coupling of localized and propagating modes makes possible to achieve large absorptance. The purpose of present study was to optimize plasmonic structure integrated superconducting nanowire single-photon detector configurations taking into account constraints that ensure experimental realization.

2. Methods

Integrated SNSPDs were designed, which consist of meandered absorbing niobium-nitride (NbN) patterns on silica substrate, capable of ensuring fabrication.

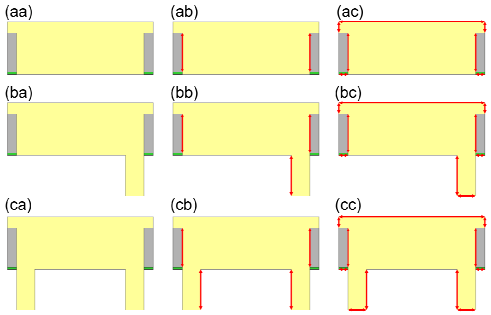

Figure 1. Inspected plasmonic structure integrated single photon-detector designs: (aa, ab, ac) nano-cavity-array (NCAI), (ba, bb, bc) nano-cavity-deflector-array (NCDAI), and (ca, cb, cc) nano-cavity-double-deflector-array (NCDDAI) integrated SNSPD. Reference (a-c/a), partially (a-c/b) and (a-c/c) completely varied geometry.

Three designs were inspected (1) nano-cavity-array (NCAI-SNSPD, Figure 1a), (2) nano-cavity-deflector-array (NCDAI-SNSPD, Figure 1b) and (3) nano-cavity-double-deflector-array (NCDDAI-SNSPD, Figure 1c) integrated devices. In reference devices the integrated patterns' periodicity was set to the P=792 nm three-quarter-wavelength of SPPs propagating at gold-silica interface, and the length of HSQ filled nano-cavities and deflectors was h=220 nm quarter-wavelength of MIM modes excitable in a single HSQ channel in gold (Figure 1 a-c/a). The w=100 nm NbN stripes width and the t=60 nm closing gold reflector thickness was also fixed, to ensure comparison with our previous studies. The deflector parameters were set according to the literature about plasmonic mirrors [14].
In partial optimization study the length of the HSQ filled cavities and of the gold deflectors was optimized, while the double deflectors' length was kept equal to promote fabrication (Figure 1a-c/b). In complete optimization all parameters were varied, while the periodicity was kept inside [750 nm, 850 nm] interval.

3. Use of COMSOL Multiphysics

RF module of COMSOL 4.4 was applied to determine the optical response and near-field distribution in case of p-polarized 1550 nm light illumination of integrated SNSPD devices in conical mounting applying the method described in our previous papers (Figures 2-4) [4, 5, 11, 12]. In case of reference SNSPDs, a parametric sweep was performed to determine the optimal orientation of these devices. In partial and complete optimization procedures the optimal structure and the optimal orientation were determined by varying the geometrical parameters and polar angle parallel. Finally, the spectral sensitivity of devices was also inspected, by performing sweeps above the wavelength and polar angle parameter space. The wavelength dependent absorptance at tilting corresponding to maxima at 1550 nm was computed and finally dispersion characteristics of all devices with parameters determined by complete optimization was inspected.

The optimization via COMSOL was performed by adding optimization study step to the RF module, and by applying the built in Monte-Carlo and Nelder-Mead algorithms in two steps, each with 500 iterations.

After that the GLOBAL optimization method was used via LiveLink for MATLAB. The GLOBAL optimization methodology is based on a special algorithm sequence, which includes sampling (Monte-Carlo), clustering (Single-link) and local search (UNIRANDI, random walk, BFGS) [15]. Finally the comparative study of the orientation and wavelength dependent absorptances of reference devices, and devices with parameters determined by partial and complete optimization via COMSOL and GLOBAL was performed.

4. Results

Comparative study of reference and optimized SNSPDs' optical responses has shown that the optimal azimuthal orientation of each devices is S-orientation (γ=90° azimuthal angle). However, several percent NbN absorptance increase can be achieved already in partially optimized configurations (Fig. 2-4, Table 1).

In NCAI-SNSPDs features corresponding to Wood anomaly appear at small tilting [11, 12, 16], while the maximal absorptance is achieved at large tilting corresponding to the plasmonic Brewster angle (PBA) [17] (Figure 2). Complete optimization performed via GLOBAL results in significantly different optical response of an integrated device with 836.18 nm periodicity at small tilting, while the highest 74.96% absorptance is reached at PBA (82.24°).

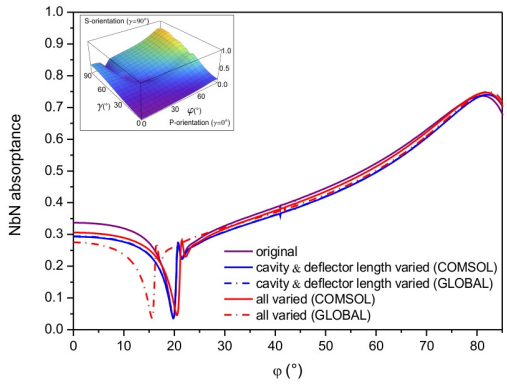

Figure 2. NbN absorptance as a function of φ polar angle in S-orientation (γ=90°) of NCAI-SNSPD designs: reference (solid gray line), partially (COMSOL/GLOBAL: solid/dash dot blue lines) and completely (COMSOL / GLOBAL: solid/dash dot red line) optimized. Inset: polar and azimuthal angle dependent NbN absorptance of NCAI-SNSPD determined by complete optimization via GLOBAL.

In reference NCDAI-SNSPD and in devices determined by partial optimization the absorptance maxima appear at similar (19.20°, 18.37° and 18.68°) tilting and the achieved absorptance is increased from 78.22% to 79.72% and 79.52% by applying COMSOL and GLOBAL methodology, respectively (Figure 3). Two successive algorithms in COMSOL results in higher absorptance. In NCDAI-SNSPDs determined by complete optimization via COMSOL and GLOBAL perpendicular incidence corresponds to maximal absorptance of 93.26% and 93.34%. This indicates that by varying all geometrical parameters, different nanophotonical phenomena are at play, and the advantages of GLOBAL become visible.

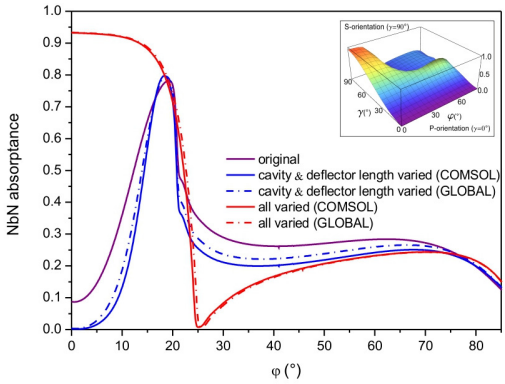

Figure 3. NbN absorptance as a function of φ polar angle in S-orientation (γ=90°) of NCDAI-SNSPD: reference (solid gray line), partially (COMSOL/GLOBAL: solid/dash dot blue line), and completely (COMSOL / GLOBAL: solid/dash dot red line) optimized. Inset: polar and azimuthal angle dependent NbN absorptance of NCDAI-SNSPD determined by complete optimization via GLOBAL.

There is no significant difference between tilting resulting in maximal absorptance in NCDDAI-SNSPDs (Figure 4). At 19.8° polar angle 86.84% and same 89.9% absorptance is attainable in the reference device, and in NCDDAI-SNSPDs determined by partial optimization via COMSOL and GLOBAL, respectively. Although partial optimization is capable of resulting in larger absorptance, the FWHM is smaller indicating that these systems would require precious orientation. Complete optimization via COMSOL/GLOBAL results in significantly larger 92.87% / 94.34% absorptance at 18.89°/21.85° tilting. Important advantage is that large absorptance can be achieved in wide polar angle interval. The advantage of GLOBAL is unambiguous, when all parameters are varied.

The maxima and FWHM of absorptance peaks sensitively depend on the optimization methodology, indicating that device optimization have to be performed taking into account requirements of specific applications.

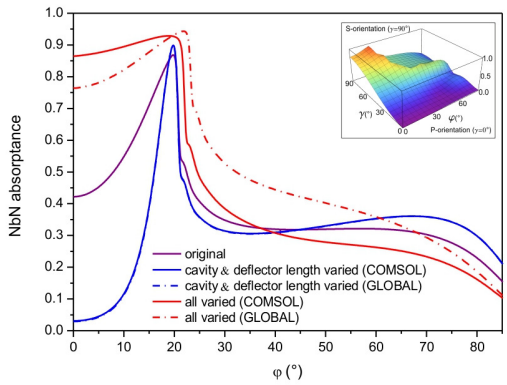

Figure 4. NbN absorptance as a function of φ polar angle in S-orientation (γ=90°) of NCDDAI-SNSPD: reference (solid gray line), partially (COMSOL / GLOBAL: solid/dash dot blue line), and completely (COMSOL/GLOBAL: solid/dash dot red line) optimized. Inset: polar and azimuthal dependent NbN absorptance of NCDDAI-SNSPD determined by complete optimization via GLOBAL.

The results of spectral sensitivity inspection indicate that the NbN absorptance in NCDAI-SNSPD at the PBA tilting, corresponding global maximum at 1550 nm, is almost wavelength independent [17] (Figure 5).

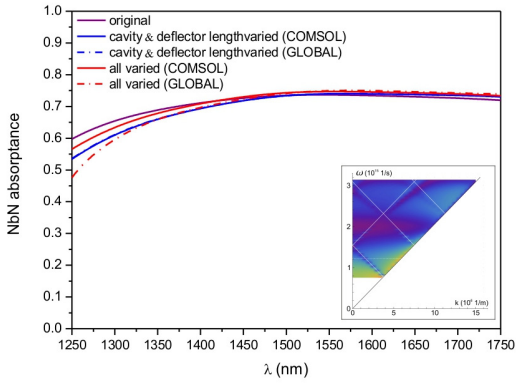

Figure 5. Wavelength dependent NbN absorptance at tilting of NCAI-SNSPDs corresponding to maximum at 1550 nm: reference (solid gray line), partially (COMSOL / GLOBAL: solid/dash dot blue line), and completely (COMSOL / GLOBAL: solid/dash dot red line) optimized. Inset: dispersion relation of NCAI-SNSPD determined by complete optimization via GLOBAL.

The dispersion curve of the device determined by complete optimization via GLOBAL indicates that the strong NbN absorption modulation at small tilting originates from the pseudo plasmonic band-gap at 1550 nm [11, 12, 18] (Inset in Figure 5).
In reference NCDAI-SNSPD and in devices determined by partial optimization via COMSOL and GLOBAL, a well defined absorption maximum appears at 1550 nm, while in devices with geometry determined by complete optimization the absorption is almost wavelength independently large (Figure 6).

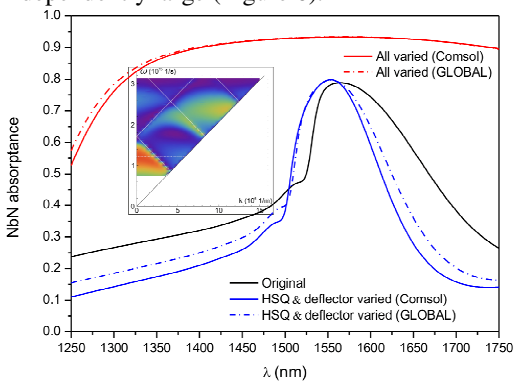

Figure 6. Wavelength dependent NbN absorptance at orientation of NCDAI-SNSPDs corresponding to maximum at 1550 nm: reference (solid gray line), partially (COMSOL/GLOBAL: solid/ dash dot blue line) and completely (COMSOL/GLOBAL: solid/dash dot red line) optimized. Inset: dispersion relation of NbN absorptance in NCDAI-SNSPD determined by complete optimization via GLOBAL.

The dispersion curve of the NCDAI-SNSPD with geometry determined by varying all parameters via GLOBAL optimization indicates that the almost polar angle independent absorption at perpendicular incidence is due to the extended inverted PBG appearing at 1550 nm (inset in Figure 6). These results indicate that coincidence of the absolute maximum on the dispersion map of the NbN absorptance corresponds to the optimal device configuration.
In all NCDDAI-SNSPD devices a large global NbN absorptance maximum appears at 1550 nm. The spectral width is intermediate in the reference device, the narrowest peak appear in devices determined by partial optimization, while the largest FWHM corresponds to devices with completely optimized geometry (Figure 7).

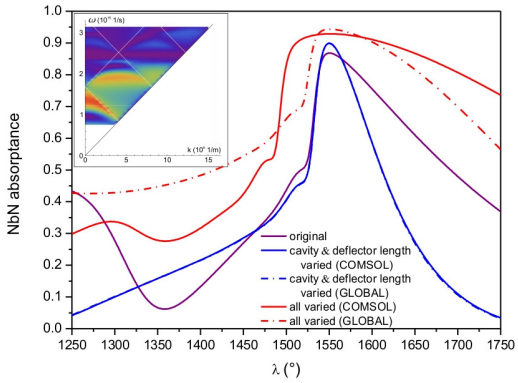

Figure 7. Wavelength dependent NbN absorptance at orientation of NCDDAI-SNSPDs corresponding to maximum at 1550 nm: reference (solid gray line), partially (COMSOL/GLOBAL: solid/dash dot blue line), and completely (COMSOL/GLOBAL: solid/dash dot red line) optimized. Inset: dispersion relation of NCDDAI-SNSPD determined by complete optimization via GLOBAL.

The dispersion curve of the NCDDAI-SNSPD device with geometry determined by complete optimization via GLOBAL indicates that the large absorptance maximum at small tilting is due to the inverted and confined PBG appearing at 1550 nm (inset in Figure 7).

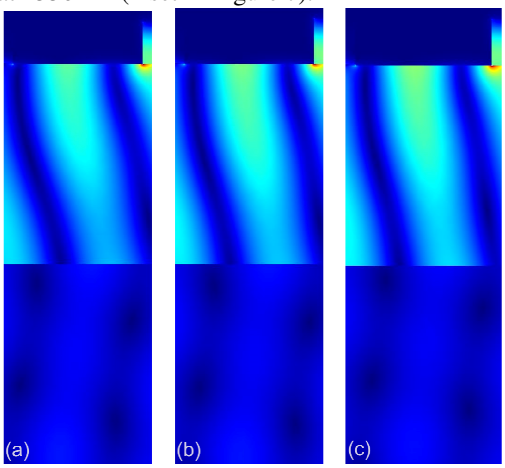

Figure 8. Near-field of NCAI-SNSPD at PBA corresponding to global maximum at 1550 nm (a) reference, (b) partially and (c) completely optimized device determined via GLOBAL.

At the optimal orientation of NCAI-SNSPDs the **E**-field is enhanced due to localized resonances in quarter wavelength cavities, and due to forward propagating waves at PBA (Figure 8).

Larger **E**-field enhancement is attainable via cavities with optimized length and via complete optimization (Figure 8b, c to a).

At the optimal orientation of NCDAI-SNSPDs the **E**-field is enhanced due to localized resonances in quarter wavelength cavities. In addition to this in the reference device and in the device determined by partial optimization backward propagating waves coupled on the periodic array result in significant **E**-field enhancement alternately in neighboring cavities (Figure 9a, b). In contrast, there are no back-reflected waves at perpendicular incidence onto devices with geometry determined by complete optimization (Figure 9c).

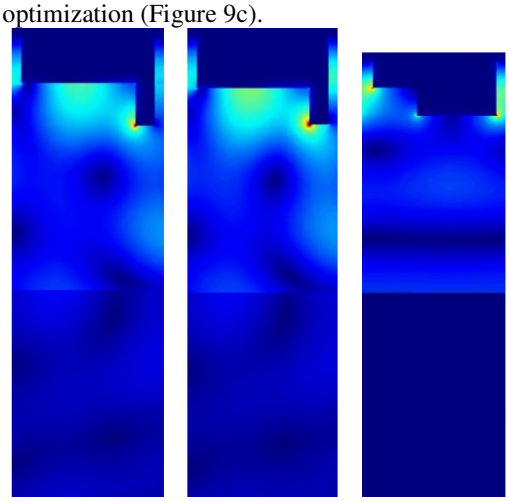

Figure 9. Near-field of NCDAI-SNSPD at orientation corresponding to global maximum at 1550 nm in (a) reference, (b) partially and (c) completely optimized device determined via GLOBAL.

At the global maxima in NCDDAI-SNSPDs the **E**-field is enhanced due to antinodes at the entrance of quarter-wavelength nano-cavities. In addition to this, the backward propagating waves coupled by the integrated structure ensure illumination of the neighboring cavities alternately. As a result, larger and the highest **E**-field is observable in NCDDAI-SNSPD with geometry determined by partial and complete optimization (Figure 10). Although, fabrication of asymmetric deflector arrays is challenging, it is a reasonable effort taking into account that 7.5% absorptance enhancement can be achieved with respect to the reference device.

The GLOBAL optimization results in asymmetric deflectors, which can be fabricated, while the second deflector determined via COMSOL is unrealistically narrow.

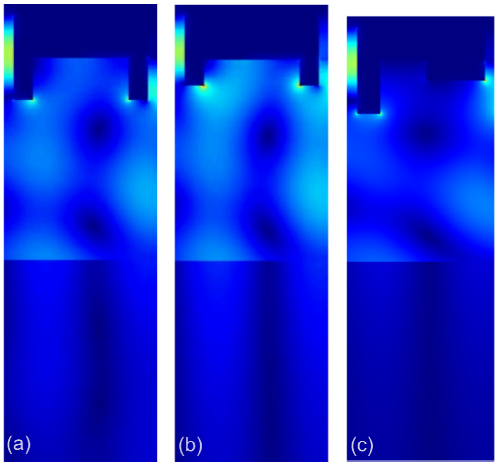

Figure 10. Near-field of NCDDAI-SNSPD at orientation corresponding to global maximum at 1550 nm (a) reference, (b) partially and (c) completely optimized device determined via GLOBAL.

5. Conclusions

Optimization of integrated plasmonic structures' makes possible to achieve larger single-photon absorptance, already in case of large number of unvaried geometrical parameters determined by users and limits of fabrication. The most efficient optimization can be realized by performing complete optimization and by using a special algorithm (GLOBAL) and monitoring modifications in the band structure.

References

1. M. S. Tame, K. R. McEnery, S. K. Özdemir, J. Lee, S. A. Maier, M. S. Kim: Quantum plasmonics, *Nature Physics* **9**, 329-340 (2013).

2. G. N. Gol'tsman, O. Okunev, G. Chulkova, A. Lipatov, A. Semenov, K. Smirnov, B. Voronov, A. Dzardanov, C. Williams and Roman Sobolewski: Picosecond superconducting single-photon optical detector, *Appl. Phys. Lett.* **79**, 705 (2001).

3. K. M. Rosfjord, J. K. W. Yang, E. A. Dauler, A. J. Kerman, V. Anant, B. M. Voronov, G. N. Gol'tsman, and K. K. Berggren: Nanowire Single-photon detector with an integrated optical cavity and anti-reflection coating, *Optics Express* **14**, 527-534 (2006).

4. M. Csete, Á. Sipos, F. Najafi, X. Hu, and K. K. Berggren: Numerical method to optimize the polar-azimuthal orientation of infrared superconducting-nanowire single-photon detectors, *Applied Optics* **50/29**, 5949 (2011).

5. M. Csete, Á. Sipos, F. Najafi, and K. K. Berggren: Optimized polar-azimuthal orientations for polarized light illumination of different superconducting nanowire single-photon detector designs, *Journal of Nanophotonics* **6/1**, 063523 (2012).
6. E. F. C. Driessen: Single-photon detectors: Fast and efficient, *Nature Photonics* **7**, 168-169 (2013).
7. F. Marsili, V. B. Verma, J. A. Stern, S. Harrington, A. E. Lita, T. Gerrits, I. Vayshenker, B. Baek, M. D. Shaw, R. P. Mirin & S. W. Nam: Detecting single infrared photons with 93% system efficiency, *Nature Photonics* **7**, 210–214 (2013).
8. W. H. P. Pernice, C. Schuck, O. Minaeva, M. Li, G. N. Goltsman, A. V. Sergienko & H. X. Tang: High-speed and high-efficiency travelling wave single-photon detectors embedded in nanophotonic circuits, *Nature Communications* **3**, (2012).
9. X. Hu, C. W. Holzwarth, D. Masciarelli, E. A. Dauler, K. K. Berggren: Efficiently Coupling Light to Superconducting Nanowire Single-Photon Detectors, *IEEE Transactions on Applied Superconductivity* **19**, 336-340 (2009).
10. X. Hu, E. A. Dauler, R. J. Molnar, K. K. Berggren: Superconducting nanowire single-photon detectors integrated with optical nano-antennae, *Optics Express* **19(1)**, 17-31 (2011).
11. M. Csete, Á. Sipos, A. Szalai, G. Szabó: Impact of polar-azimuthal illumination angles on efficiency of nano-cavity-array integrated single-photon detectors, *Optics Express* **20/15**, 17067 (2012).
12. M. Csete, Á. Sipos, A. Szalai, G. Szekeres, F. Najafi, G. Szabó, K. K. Berggren: Improvement of infrared single-photon detectors absorptance by integrated plasmonic structures, *Scientific Reports* **3**, 2406 (2013).
13. R. W. Heeres, S. N. Dorenbos, B. Koene, G. S. Solomon, L. P. Kouwenhoven and V. Zwiller: On-Chip Single Plasmon Detection, *Nano Letters* **10(2)**, 661–664 (2010).
14. A. Sánchez-Gil & A. A. Maradudin: Near-field and far-field scattering of surface plasmon polaritons by one-dimensional surface defects, *Physical Review B* **60**, 8359 (1999).
15. T. Csendes, L. Pál, J. O. H. Sendín, J. R. Banga: The GLOBAL Optimization Method Revisited, *Optimization Letters* **2**, 445-454 (2008).
16. R. W. Wood: Anomalous Diffraction Gratings, *Physical Review* **48**, 928–937 (1935).
17. A. Alù, G. D'Aguanno, N. Mattiucci, and M. J. Bloemer: Plasmonic Brewster Angle: Broadband Extraordinary Transmission through Optical Gratings, *Phys. Rev. Lett.* **106**, 123902 (2011).
18. D. de Ceglia, M. A. Vincenti, M. Scalora, N. Akozbek, & M. J. Bloemer, "Plasmonic band edge effects on the transmission properties of metal gratings," AIP Advances **1** (3), 032151 (2011).

Table 1: Illumination direction dependent NbN absorptance

NCAI	$\phi(°)$	*NbN Abs*
Reference	**81**	**73.66%**
HSQ varied (Comsol)	**82.08**	**74.00%**
HSQ varied (GLOBAL)	**82.01**	**74.00%**
All varied (Comsol)	**81.72**	**74.70%**
All varied (GLOBAL)	**82.24**	**74.96%**

NCDAI	$\phi(°)$	*NbN Abs*
Reference	**19.2**	**78.22%**
HSQ varied (Comsol)	**18.37**	**79.72%**
HSQ varied (GLOBAL)	**18.68**	**79.52%**
All varied (Comsol)	**0**	**93.26%**
All varied (GLOBAL)	**0**	**93.34%**

NCDDAI	$\phi(°)$	*NbN Abs*
Reference	**19.8**	**86.84%**
HSQ varied (Comsol)	**19.8**	**89.90%**
HSQ varied (GLOBAL)	**19.79**	**89.90%**
All varied (Comsol)	**18.89**	**92.87%**
All varied (GLOBAL)	**21.85**	**94.34%**

Acknowledgements

The authors would like to thank Francesco Marsili at JPL, Sae Woo Nam and Varun Verma at NIST for the helpful discussions. This work was partially supported by the European Union and the European Social Fund through project "Supercomputer, the national virtual lab" (grant no.: TÁMOP-4.2.2.C-11/1/KONV-2012-0010) and "Impulse lasers for use in materials science and biophotonics" (grant no.: TÁMOP-4.2.2.A-11/1/KONV-2012-0060).